ENVIRONMENTAL RESEARCH
LETTERS

CrossMark

OPEN ACCESS

RECEIVED
5 March 2024

REVISED
5 July 2024

ACCEPTED FOR PUBLICATION
19 July 2024

PUBLISHED
19 August 2024

Original content from this work may be used under the terms of the Creative Commons Attribution 4.0 licence.

Any further distribution of this work must maintain attribution to the author(s) and the title of the work, journal citation and DOI.

LETTER

Projected impact of solar radiation modification geoengineering on water deficit risk over major Central African river basins

Thierry C Fotso-Nguemo[1,2,*], Steven Chouto[1,3], Jean P Nghonda[1,3], Arona Diedhiou[2,4], Ben Kravitz[5,6], Zéphirin D Yepdo[1], Flore K Djuidje[1,7] and Babatunde J Abiodun[8,9]

1 Climate Change Research Laboratory (CCRL), National Institute of Cartography, PO Box 157, Yaounde, Cameroon
2 Laboratoire Mixte International 'Nexus sur les Interrelations Climat, Eau, Agriculture et Énergie en Afrique et le Développement de Services Climatiques' (LMI NEXUS), Université Félix Houphouët-Boigny, PO Box 463, Abidjan, Ivory Coast
3 Department of Geography, Higher Teacher Training College, University of Maroua, PO Box 55, Maroua, Cameroon
4 University of Grenoble Alpes, IRD, CNRS, Grenoble INP, IGE, 38000 Grenoble, France
5 Department of Earth and Atmospheric Sciences, Indiana University, Bloomington, IN, United States of America
6 Atmospheric, Climate, and Earth Sciences Division, Pacific Northwest National Laboratory, Richland, WA, United States of America
7 Department of Geography, Faculty of Arts Letters and Social Sciences, University of Yaounde 1, PO Box 755, Yaounde, Cameroon
8 Climate Systems Analysis Group, Department of Environmental and Geographical Science, University of Cape Town, Cape Town, South Africa
9 Nansen-Tutu Centre for Marine Environmental Research, Department of Oceanography, University of Cape Town, Cape Town, South Africa
* Author to whom any correspondence should be addressed.

E-mail: fotso.nguemo@gmail.com

Keywords: central africa, water deficit, climate change, SRM

Supplementary material for this article is available online

Abstract

The economy of Central African countries strongly depends on rain-fed agriculture and hydropower generation. However, most countries in this subregion do not yet have the irrigation technologies that are already applied in many more advanced nations, which further exposes them to the serious risk of severe drought caused by global warming. This study investigates the potential impact of solar radiation modification (SRM) geoengineering on the water availability over the four major river basins that cross most of Central African countries (i.e. Niger Basin, Lake Chad Basin, Cameroon Atlantic Basin (CAB) and Congo Basin). For this purpose a potential water availability index was computed based on an ensemble-mean simulations carried out in the framework of Phase 6 of the Geoengineering Model Intercomparison Project considering two SRM simulation experiments: the stratospheric sulphate aerosol injection (G6sulfur) and the global solar dimming (G6solar). The climate change simulation results in a robust decreases by up to 60% in water availability, most pronounced over the CAB under the high radiative forcing scenario. Therefore, in a business-as-usual world, the reduction in water availability combined with the rapid population growth expected by 2050 in the studied subregion, could result in a significant water deficit over Central African countries towards the end of the 21st century. This water deficit could affect all activities that depend on water resources, such as water supply, agriculture and hydropower generation. Furthermore, the results also show that SRM methods have the potential to significantly reduce this deficit by increasing water availability (as compared to climate change) by up to 50% over the affected river basins, with a more accentuated increase found in the CAB when the global solar dimming is applied. These results suggest good possibilities of adaptation for populations living in the geographical areas of these river basins.

© 2024 The Author(s). Published by IOP Publishing Ltd

1. Introduction

Central Africa is characterized by its unique and diverse ecosystems, crossed by vast river basins that are vital sources of water for populations living there. However, the growing threat of climate change poses significant challenges to the subregion's water resources, especially as climate projections indicate an increased risk of water deficits and associated impacts on agriculture, biodiversity and livelihoods of populations (IPCC 2022).

Therefore, scientists, civil society and policymakers have explored various strategies to mitigate the effects of global warming. One of these is solar radiation modification (SRM) geoengineering (Kravitz *et al* 2011, Latham *et al* 2012, Alterskjær *et al* 2013, Muri *et al* 2014, Storelvmo *et al* 2014), which involves manipulating the Earth's radiation budget to counteract some of the warming effects caused by greenhouse gas (GHG) emissions. Accordingly, the implementation of SRM is based on several approaches including: (i) marine cloud brightening, which involves spraying seawater into low-level marine clouds to produce smaller droplets and make them more reflective (e.g. Latham *et al* 2012, Alterskjær *et al* 2013); (ii) cirrus cloud thinning, involves modification of cirrus cloud properties by seeding them to produce crystals that reduce their ability to trap heat (e.g. Muri *et al* 2014, Storelvmo *et al* 2014); (iii) global solar dimming (GSD), which consists of deploying large structures in space that can reflect a portion of incoming sunlight back to space before it reaches the Earth (e.g. Tilmes *et al* 2022, Xie *et al* 2022) and (iv) stratospheric aerosol injection (SAI), which is the most widely discussed technique in the literature and consists of creating reflective aerosols (e.g. sulfate) in the stratosphere (15–30 km high) in order to mimic large volcanic eruptions (e.g. Pinto *et al* 2020, Odoulami *et al* 2020, Abiodun *et al* 2021, Camilloni *et al* 2022, Bonou *et al* 2023, Obahoundje *et al* 2023, Tan *et al* 2023).

To date, research on the effects of SRM on climate has focused on regional (Robock *et al* 2008, Pinto *et al* 2020) and global (Aswathy *et al* 2015, Dagon and Schrag 2016) perspectives, highlighting that interventions to maintain global warming at an acceptable level could lead to diverse climate results. Therefore, while some studies have shown that although the SRM does not restore the global climate to its pre-warming state, it has the potential to decrease global surface temperature and thus significantly reduce extreme weather events (e.g. floods, droughts, heat waves and heat stress) over many parts of the world, including Africa (Pinto *et al* 2020, Odoulami *et al* 2020, Abiodun *et al* 2021, Bonou *et al* 2023, Obahoundje *et al* 2023), Asia (Kuswanto *et al* 2022, Tan *et al* 2023), as well as Europe and America (Aswathy *et al* 2015, Dagon and Schrag 2016, Xu *et al* 2020, Camilloni *et al* 2022).

However, although some of these studies have assessed drought risk in Africa, they have mainly focused their attention on the evaluation of the implications of the possible use of SAI over specific subregions of Africa (Pinto *et al* 2020, Odoulami *et al* 2020, Abiodun *et al* 2021). Therefore, this study investigates the potential impact of SRM on the risk of water deficit over the main Central African river basins, by considering two different SRM approaches (i.e. GSD and SAI). Based on an ensembles of global climate models (GCMs) built from experiments derived from Phase 6 of the Coupled Model Intercomparison Project (CMIP6; Eyring *et al* 2016), and Phase 6 of the Geoengineering Model Intercomparison Project (GeoMIP6; Kravitz *et al* 2015), we seek to highlight the potential benefits, risks and uncertainties associated with this controversial approach, by quantifying the impact of climate change on potential water availability taking into account precipitation and potential evapotranspiration over each river basin. Understanding the potential implications of SRM on water resources over the Central African river basins is crucial for providing valuable insights for climate resilience and sustainable water management under a changing climate.

It is worth noting that this study does not argue for or against SRM as a solution to climate change. Instead, its aim is to contribute to the current scientific discourse on climate geoengineering and its potential implications for water resources in the Central African subregion. By promoting a better understanding of the potential risks and benefits, we can facilitate informed policy discussions and decisions that prioritize the long-term sustainability and resilience of Central African river basins in the face of a rapidly changing climate.

Overall, this study could be a valuable contribution to enhance our understanding of climate change, geoengineering and water resources over Central Africa. By examining the predicted impact of the SRM geoengineering on the water deficit risk, we hope to provide a sound basis for further research and informed decision-making in the pursuit of a climate-resilient future for the region. The rest of this paper is structured as follows: First, the datasets and methodology used in the study are described in section 2. The results are presented in section 3. Finally, the main results are discussed and concluded in section 4.

2. Data used and methodology

For the analyses of the potential changes in hydroclimatic variations over the main Central African river basins, we considered monthly data from an ensemble-mean of six GCMs simulations members, extracted from the archives from CMIP6 and GeoMIP6 initiatives (Kravitz *et al* 2015, Eyring *et al* 2016). However, given that the GeoMIP6 archives currently only have six models available, this study

Table 1. Summary of the six GCMs used in the framework of the CMIP6 and GeoMIP6 initiatives.

Model name		Institute ID	Resolution (Lon × Lat)	References
1	CESM2-WACCM	National Center for Atmospheric Research, Boulder, USA	1.25° × 0.94°	Danabasoglu (2019)
2	CNRM-ESM2-1	Centre National de Recherches Météorologiques, Météo-France, Toulouse, France	1.41° × 1.41°	Séférian *et al* (2019)
3	IPSL-CM6A-LR	Institut Pierre Simon Laplace, Paris, France	2.50° × 1.27°	Boucher *et al* (2020)
4	MPI-ESM1-2-HR	Max Planck Institute for Meteorology, Hamburg, Germany	0.94° × 0.94°	Müller *et al* (2018)
5	MPI-ESM1-2-LR	Max Planck Institute for Meteorology, Hamburg, Germany	1.88° × 1.88°	Schupfner *et al* (2021)
6	UKESM1-0-LL	Met Office Hadley Centre, Exeter, UK	1.88° × 1.25°	Tang *et al* (2019)

is therefore limited to the number of GCMs simulations accessible simultaneously in the CMIP6 and GeoMIP6 archives (see, table 1 for the summary of different GCMs simulations used). It is worth noting that historical data covering the 1850–2014 period is only available for CMIP6 models, while future projections over the 2015–2100 period are available for both CMIP6 and GeoMIP6 models.

In this work, the future changes for the CMIP6 simulations are projected under two Shared Socioeconomic Pathways (SSPs; O'Neill *et al* 2017) scenarios: SSP2-4.5 and SSP5-8.5. Here, SSP5-8.5 represents a business-as-usual world and thus a high-level forcing scenario, whereas SSP2-4.5 considers some GHG mitigation and is thus a mid-level forcing scenario. Moreover, the future changes for the GeoMIP6 ensemble-mean are projected under two SRM scenarios: G6sulfur which corresponds to the SAI approach and G6solar which is linked to the GSD technique (Kravitz *et al* 2015). In fact, G6sulfur considers the injection of sulfur between 10°S–10°N latitude and approximately 18–20 km altitude to maintain surface temperatures at the same values as those simulated in the target scenario SSP2-4.5 (against a background of the SSP5-8.5 scenario), while G6solar consists of a reduction of the global solar constant to offset the same temperature difference in order to reach the values of the SSP2-4.5 scenario.

In this study, the estimation of the hydroclimatic changes over the main Central African river basins, were estimated by adopting an approach based on the potential water availability index, computed from the ratio between precipitation and potential evapotranspiration, which is considered as a proxy for water availability (Greve and Seneviratne 2015, Sylla *et al* 2018, Zhang *et al* 2022). In this context, precipitation is considered as a climatic water supply, while potential evapotranspiration as a climatic water demand. Therefore, when the potential water availability index is greater than 1 (i.e. precipitation greater than potential evapotranspiration), the basin is likely to gain more water than it would lose and therefore undergo water surplus, and vice-versa.

Concerning the computation of the potential evapotranspiration, several studies have highlighted the presence of uncertainties in the different methodologies used for its estimation, especially when it involves the study of future climate (Kingston *et al* 2009, Wang *et al* 2017, Kadkhodazadeh *et al* 2022). Consequently, for this study, the potential evapotranspiration was derived according to the Hamon's method, as it was found to be closer to observations under different African climates (Lhomme 1997, Lu *et al* 2005, Terzi and Keskin 2010, Sylla *et al* 2016, Owusu-Sekyere *et al* 2017). In fact, the Hamon's formulation enables an estimation of the potential evapotranspiration based on the monthly mean near-surface temperature and the day length (Hamon 1963, Lu *et al* 2005). Its mathematical formulation is expressed as follows:

$$\mathrm{PET} = k \times 0.1651 \times L_{\mathrm{day}} \times \varrho_{\mathrm{sat}} \tag{1}$$

$$\varrho_{\mathrm{sat}} = \frac{216.7 \times e_s}{(T + 273.3)} \tag{2}$$

$$e_s = 6.108 \times e^{\left(\frac{17.27 \times T}{T + 237.3}\right)} \tag{3}$$

where,

PET: monthly potential evapotranspiration [mm]
k: proportionality coefficient = 1[1] [unitless]
L_{day}: daytime length [x/12 h]
ϱ_{sat}: saturated vapor density [g m^{-3}]
e_s: saturation vapor pressure [mb]
T: monthly mean near-surface temperature [°C]

Therefore, for each GCMs experiment, the potential water availability index was derived for a three 30 year time slice periods chosen as follows: one reference (1985–2014) representing the baseline period, and two futures (2021–2050 and 2071–2100) representing the near and far future, respectively. Changes in the water availability index were expressed in %, with respect to the baseline period, and is computed as follows: first of all, for analyses of spatial distributions, a temporal average was calculated for each grid cell fields of the considered variables, then their difference with respect to the spatio-temporal

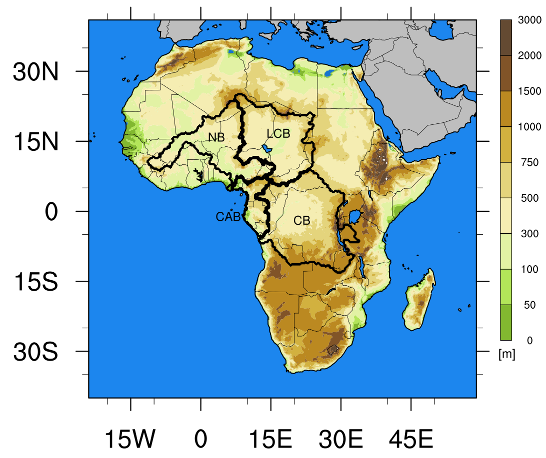

Figure 1. Mean topography (in meter; shaded) of the African domain. Outlines in bold delineate the contour of the main Central African river basins, including: Niger Basin (NB), Lake Chad Basin (LCB), Cameroon Atlantic Basin (CAB) and Congo Basin (CB).

average of the reference variable was computed and expressed as a percentage. Secondly, in the case of analyses at watershed scale, a spatial average was performed beforehand for each grid cell fields of the considered variables, then their difference with respect to the spatio-temporal average of the reference variable was calculated and expressed as a percentage. Furthermore, the analysis of spatial distributions will be carried out over the African continent with a focus on the main Central African river basins, as illustrated in figure 1. However, regional analyses will be performed at the scale of each river basin, including: Niger Basin (NB), Lake Chad Basin (LCB), Cameroon Atlantic Basin (CAB) and Congo Basin (CB).

Given that the considered GCMs have different grid-spacing resolutions, an interpolation at $1^\circ \times 1^\circ$ was performed as follows: the bilinear interpolation was applied to models with a coarser resolution, while conservative techniques were used to interpolate models with a finer resolution as recommended by Jones (1999). To take into account the uncertainties that may exist in the projected changes, the climate change signal from the GCMs ensemble-mean will be considered as robust if the following two criteria are fulfilled: (i) at least five out of six (i.e. about 83.33%) models members agree on the sign of the GCMs ensemble-mean change; and (ii) the signal to noise ratio (SNR), i.e. the ratio of the mean to the standard deviation of the GCMs ensemble-mean, is equal or greater than 1. In fact, the second condition measures the climate change signal strength relative to inter-model variability. We use both the first and second criteria since the first alone could indicate consistency even for very small changes close to zero (Collins *et al* 2013). If only the first criterion is met, we describe the change as significant.

3. Results

3.1. Projected change in the spatial variability of the water availability

Figure 2 shows the spatial distribution of the changes in the annual potential water availability projected by the GCMs ensemble-mean simulations for the different basins for the baseline period, the near and far future; under the SSP2-4.5, SSP5-8.5, G6sulfur and G6solar scenarios. During the baseline period, the northern part of Sahelian river basins (i.e. NB and LCB) show a potential water availability index values generally lower than 1. On the other hand, their southern part show an average values of index between 1 and 2, reflecting moderate conditions of water availability. The CAB has higher values of index (close to 5), suggesting that water availability is generally more abundant and less variable. Concerning the CB, the results show values of index between 2 and 4, indicating abundant water resources throughout the year, probably due to heavy precipitation favored by the presence of the Congo Basin rainforest.

During the near future, the projected water availability for the main Central African river basins shows contrasting results under scenarios SSP2-4.5 and SSP5-8.5 scenarios. Indeed, a downward trend is projected under SSP2-4.5 scenario, whereas an upward trend is predominant under SSP5-8.5 scenario. For instance, a significant deceases of up to 30% under the SSP2-4.5 scenario and a robust increases of up to 40% under the SSP5-8.5 scenario, are projected by the ensemble-mean models over countries crossed by the NB, LCB and CB, with a peak located over eastern Democratic Republic of Congo (DRC). Moreover, countries crossed by the CAB show a significant increase of up to 30% under SSP2-4.5 scenario, and a significant decrease of up to 40% under the SSP5-8.5 scenario, more pronounced over southern Gabon (figures 2(b) and (d)). During the far future, the climate change signal projected by the ensemble-mean models in the context of the radiative forcing scenarios due to the increase in GHGs shows that the water reserves of countries crossed by the considered catchment tend to dry up. This drying up is mainly translated through: (i) a more pronounced reduction in water availability in the countries crossed by CAB and CB, with peaks rising from about 30% in the near future to about 50% in the far future under the SSP2-4.5 scenario (in the case of CB), and from about 40% in the near future to about 60% in the far future under SSP5-8.5 scenario (in the case of CB); (ii) a slight decrease which did not exist in the near future, is now recorded over Sahelian river basins under the SSP2-4.5 scenario, and western and southern parts of CB under SSP5-8.5 scenario; and (iii) a smaller robust increase, with peaks rising from about 40% in the near future to about 20% under under SSP5-8.5 scenario in the far future, is projected over NB, LCB

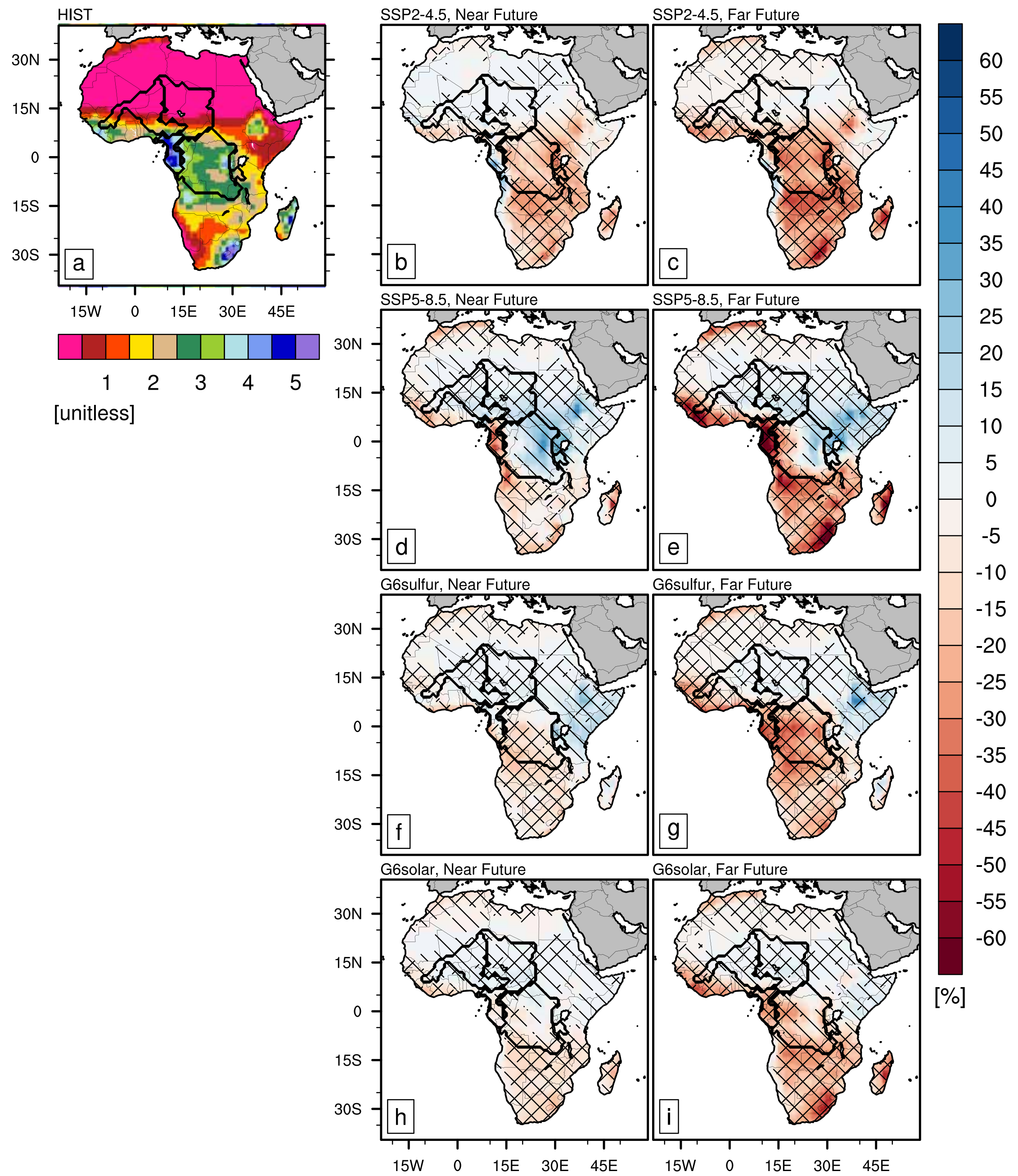

Figure 2. Spatial distribution of the annual potential water availability index, derived from the GCMs ensemble-mean simulations during the 1985–2014 baseline period (a); first column) and its change (in %, with respect to the baseline period) during the Near Future (second column) and Far Future (third column), under SSP2-4.5 (b)–(c); first row), SSP5-8.5 (d)–(e); second row), G6sulfur (f)–(g); third row) and G6solar (h)–(i); fourth row) scenarios. Outlines in bold delineate the contour of each river basin. Areas where the change is significant (i.e. where at least 5 out of 6 models members agree on the sign of the change) are highlighted by positively sloped hatching ('/'). Areas where the change is robust (i.e. where the SNR > 1) are highlighted by negatively sloped hatching ('\').

and CB (figures 2(d) and (e)). It is therefore clear that in the far future, radiative forcing due to the increase in GHGs will have the effect of accelerating the reduction in water reserves useful for plants over the countries crossed by the main Central African river basins, with CAB undergoing the most pronounced changes, especially under the SSP5-8.5 scenario (figures S1(i) and (j)).

The results of the spatial distributions of potential water availability index projected by the ensemble-mean models under the SRM scenarios (i.e. G6sulfur and G6solar) show a similar pattern to those for the SSP2-4.5 scenario presented above, but with greater spatial extent of increase. It is worth noting that in these scenarios, the amplitudes of increase are greater and those of the decrease are less than in the case of warming scenarios. For example, in the near future, the ensemble-mean models project a robust increase of up to 30% in NB, LCB and CB under the G6sulfur and G6solar scenarios as compared to the SSP2-4.5 scenario (figures S1(a) and (d)). Similarly, in the far future, the models project a significant

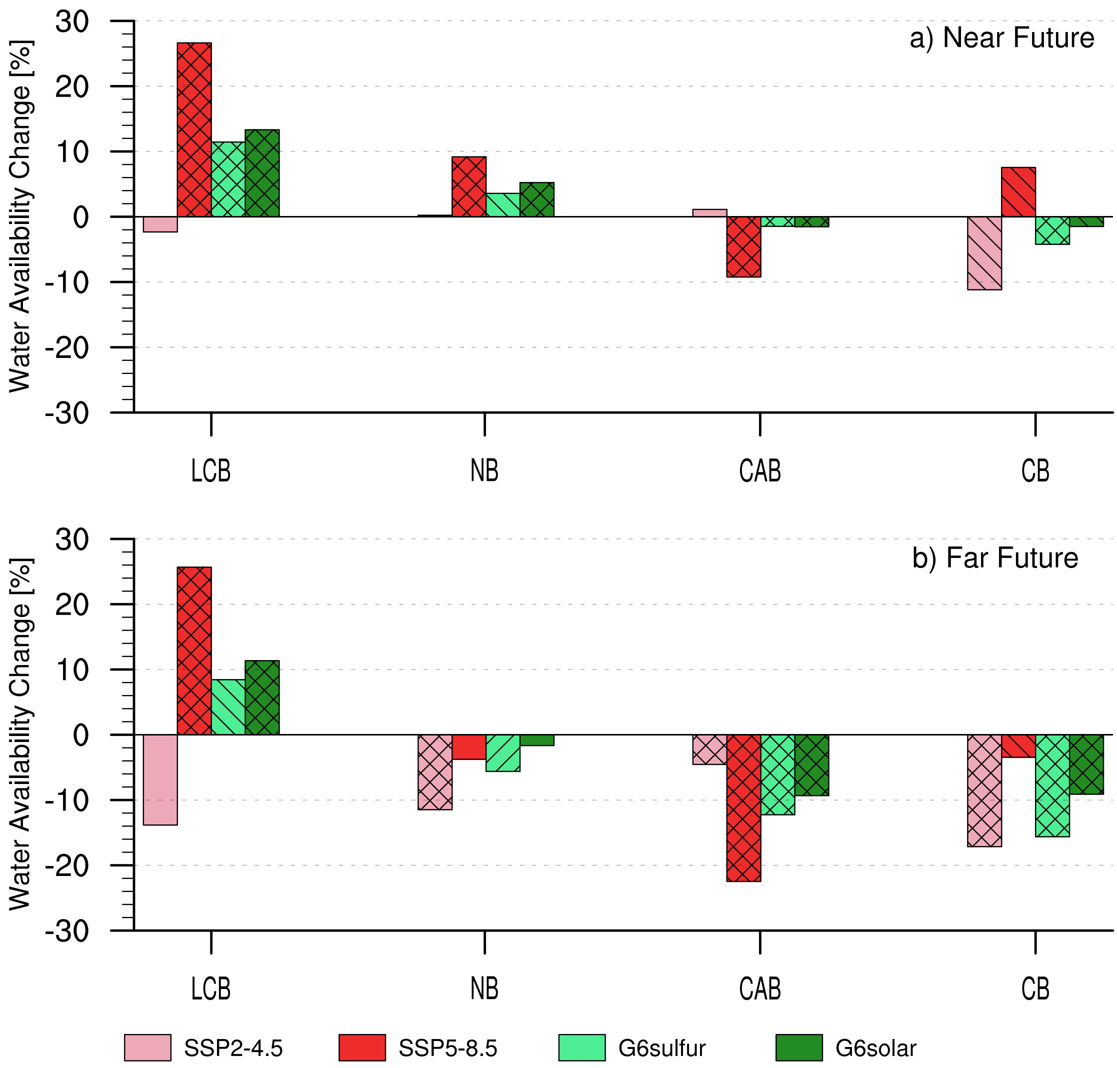

Figure 3. Changes in the annual potential water availability index (in %, with respect to the 1985–2014 baseline period) during the (a) Near Future and (b) Far Future, for each river basin as projected by the GCMs ensemble-mean simulations, under SSP2-4.5 (pink), SSP5-8.5 (red), G6sulfur (light green) and G6solar (green) scenarios. Significant changes (i.e. where at least 5 out of 6 models members agree on the sign of the change) are highlighted by positively sloped hatching ('/'). Robust changes (i.e. where the SNR > 1) are highlighted by negatively sloped hatching ('\').

increase of up to 60% in CAB under the G6sulfur and Gsolar scenarios as compared to the SSP5-8.5 scenario (figures S1(g) and (h)). A comparison between the two mitigation methods used in this study shows contrasting spatial variability (figures S1(k) and (l)). Nevertheless, the solar dimming method appears to be more effective in significantly reducing the potential deficit in water available to plants in Gabon, Congo, DRC and southern Central African Republic.

To investigate whether the changes in the annual potential water availability projected by the ensemble-mean models could lead to a risk of deficit at the scale of each catchment, their regional average has been estimated for the near and far future, as shown in figure 3. The results show that under all the considered scenarios, a systematic decrease of up to approximatively 23% is projected in CAB and CB, during the far future. Although only occurring in the far future, a decline of up to about 12% is also projected in NB. A possible explanation for this decrease in groundwater reserves would be linked to a small increase in precipitation (around 2% to 24%) coupled with a relatively large increase in potential evapotranspiration (around 14% to 29%) in these basins (figures S2 and S3). Concerning NB and LCB (located in the Sahelian part of Africa and therefore more exposed to severe drought problems), the ensemble-mean models project an increase under almost all the considered scenarios, except in the NB during the far future where a reversed trend is projected. Particularly for LCB, a robust increase in the potential water availability index was more pronounced in the near future, with up to about 27% found under the SSP5-8.5 scenario. It should be noted that in almost all the considered river basins, the water availability projected by SSP2-4.5 shows a downward trend more pronounced in the far future. Nevertheless, the SRM scenarios succeed in reversing

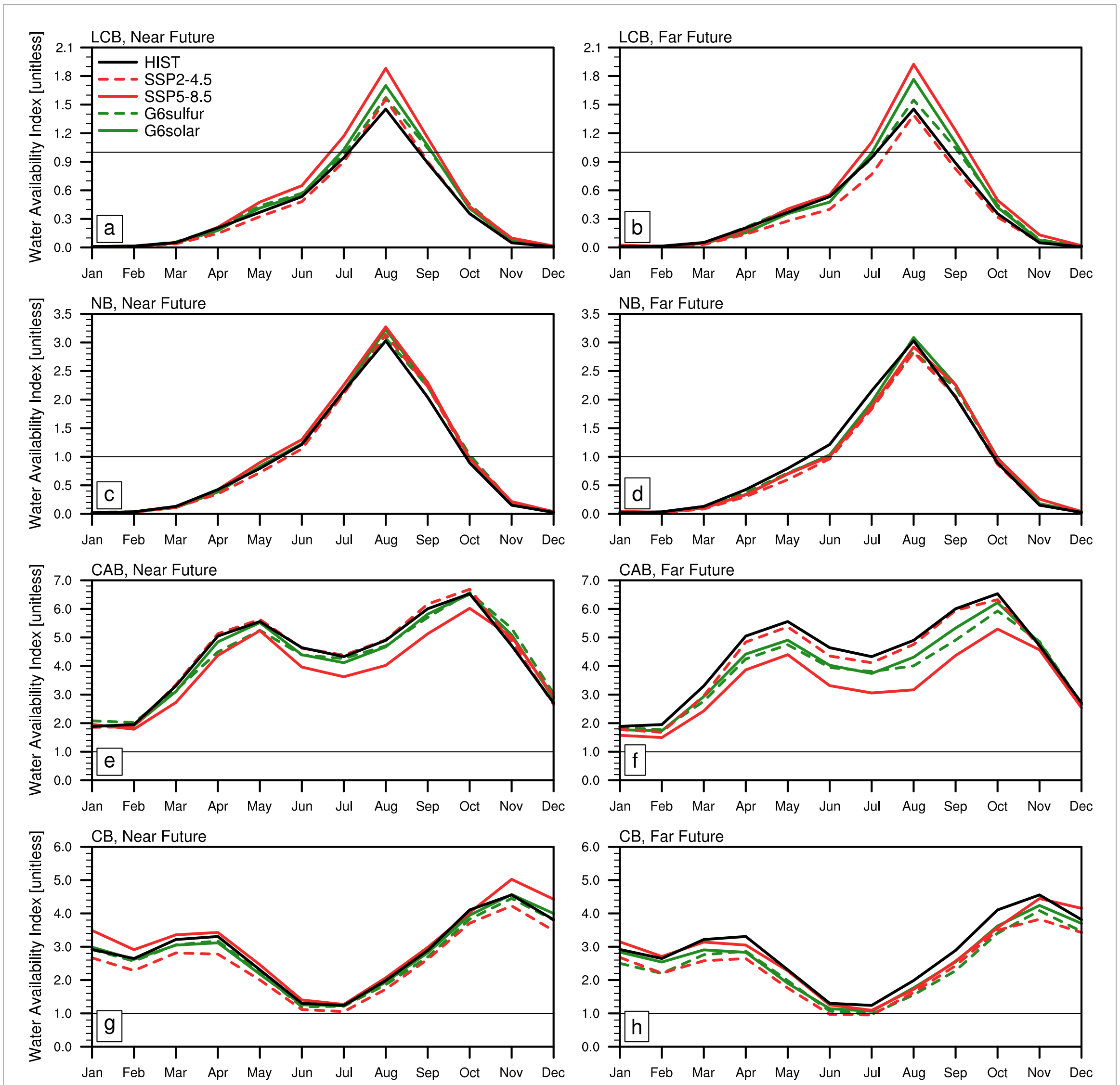

Figure 4. Annual cycle of the potential water availability index (unitless), during the Near Future (left column) and Far Future (right column), for each river basin as projected by the GCMs ensemble-mean simulations, during the baseline (black) and future periods under SSP2-4.5 (dashed red), SSP5-8.5 (solid red), G6sulfur (dashed green) and G6solar (solid green) scenarios. The horizontal line indicates the threshold above which precipitation exceeds potential evapotranspiration (i.e. where the potential water availability index = 1).

this trend by significantly increasing the water availability by up to 25% under the G6sulfur scenario and 30% under the G6solar scenario (figure S4). Furthermore, the SRM scenarios also succeed in reversing the downward trend projected in CAB, by enabling a significant increase of up to about 17% in available water (figure S4).

3.2. Projected change in the annual cycle of the water availability

In order to determine whether the negative changes found above, effectively lead to a water deficit, the annual cycle of the potential water availability index at the scale of each of the main Central African basins was analyzed during the historical and future periods under the SSP2-4.5, SSP5-8.5, G6sulfur and G6solar scenarios, as shown in figure 4. The annual variation curves of the potential water availability index over the Sahelian and forested basins for the SSP2-4.5, SSP5-8.5, G6sulfur and G6solar scenarios could provide important information on the water availability over these basins and how it could be affected by climate change.

During the reference period, for NB and LCB, which have a semi-arid climate, the potential water availability index obtained from the ensemble-mean of models shows an annual cycle with a deficit trend (i.e. index lower than 1) which has a longer duration in the case of LCB (i.e. from September to July). Although of relatively short duration compared with the total length of the year, a tendency towards a water surplus is noted in these river basins during the rainy season (i.e. from June to September), with a peak found around August (figures 4(a) and (c)). On the other hand, for CAB and CB, which are characterized by a tropical climate, the annual cycle of the potential

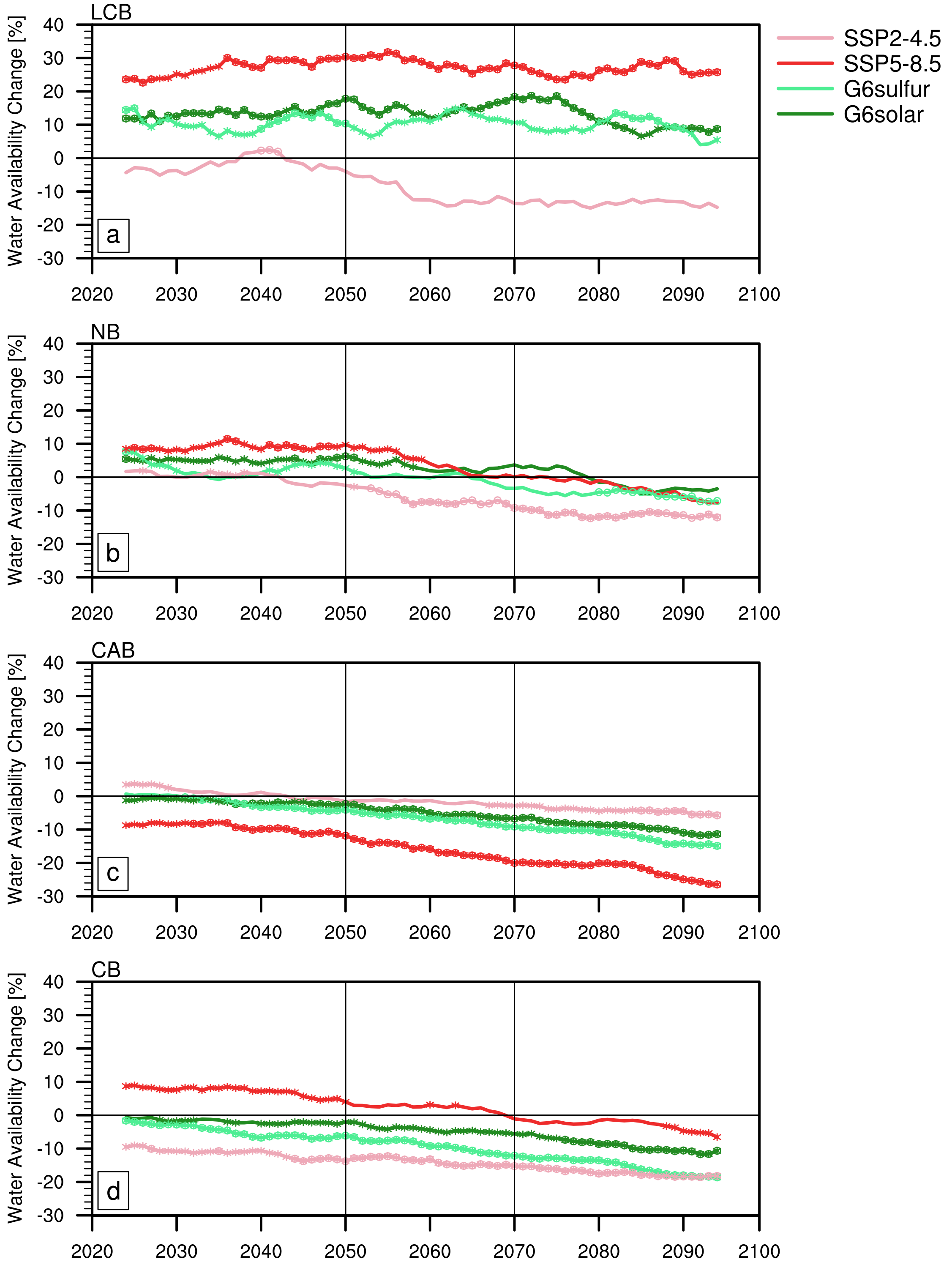

Figure 5. Time series of the year-to-year changes in the potential water availability index (in %, with respect to the 1985–2014 baseline period), for each river basin, during the future climate as projected by the GCMs ensemble-mean simulations, under SSP2-4.5 (pink), SSP5-8.5 (red), G6sulfur (light green) and G6solar (green) scenarios. Significant changes (i.e. where at least 5 out of 6 models members agree on the sign of the change) are highlighted by circles ('°'). Robust changes (i.e. where the SNR > 1) are highlighted by stars ('*'). A 10-year running average has been applied to remove high-frequency variability.

water availability index shows a tendency towards a water surplus (i.e. index greater than 1) throughout the year, with the maximum and minimum values reached during the rainy (i.e. from March to May and from September to November) and dry (i.e. from December to February and from June to August) seasons, respectively (figures 4(e) and (g)).

In the near future, the annual cycles of the potential water availability remain broadly the same under the SSP2-4.5 and SSP5-8.5 scenarios, with maximum values projected during the rainy seasons and minimum values expected during the dry seasons. There is a slight increase in the value of the water availability index in NB and LCB, and a slight decrease in CAB and CB. In the far future, the decrease in the value of the potential water availability index concerns both the peaks during the dry and rainy seasons, and is more marked under the scenario of greater radiative forcing, compared with the historical reference period. This decrease, which could translates into an increased risk of drought associated with the increased global warming, would be more marked for CAB in the far future (figure 4(f)).

With a drastic reduction in water deficit risk through SRM interventions, the results show that the G6sulfur and G6solar scenarios are able to limit this decrease in the peak of the potential water availability index projected under warming scenarios (SSP2-4.5 and SSP5-8.5), by approaching those of the median radiative forcing (SSP2-4.5), or even slightly increase them compared to the baseline period (especially for the G6solar scenario; figure 4(b)).

3.3. Projected change in the year-to-year water availability

The time series of the year-to-year changes in the potential water availability index (in % of the mean value for the baseline period) in the different river basins over the period 2020–2100 under the SSP2-4.5, SSP5-8.5, G6sulfur and G6solar scenarios are shown in figure 5. The results for LCB show a trend towards positive change under the SSP5-8.5 scenario, with a peak of around 30% occurring near 2055 until the end of the 21st century. Under the SSP2-4.5 scenario, the ensemble-mean models projects a risk of water deficit of up to around 15% found around 2058 until the end of the century. This is probably due to the increase in potential evapotranspiration projected under this scenario (up to around 16%), compared with precipitation, for which the ensemble-mean of models projects a slight decrease (see, figures S2 and S3; Chad). For this catchment, the year-to-year changes in the potential water availability index projected under the SRM scenarios showed a trend towards robust positive change throughout the 21st century, with a peak of up to 15% projected when SAI was applied, and 20% under GSD.

For the other basins, the year-to-year changes in potential water availability projected by the ensemble-mean models shows a negative trend throughout the 21st century, for all the considered scenarios. However, the results show a positive variation projected by the SSP2-4.5 scenario in NB and CAB until 2045, and by the SSP5-8.5 scenario in NB and CB until 2080. It should be pointed out that during the second half of the 21st century, the SSP2-4.5 radiative forcing scenario generally predicts a more pronounced water deficit (up to around 20%) over all the Central African river basins, except in CAB where the radiative forcing scenario SSP5-8.5 is likely to trigger a robust decrease of about 25% in water availability. Nevertheless, the magnitude of this decrease in water availability, which would be more pronounced during the second half of the 21st century in the warming scenarios, is generally reduced in the SRM scenarios and even falls below that of the SSP5-8.5 scenario after 2090 in the case of NB.

4. Discussion and conclusion

In the present study, we examined the projected impacts of the SRM on the water deficit risk over the major Central African river basins. For this purpose, we considered the projections of an index characterizing the potential availability of water by combining precipitation and potential evapotranspiration which was applied to an ensemble mean of six GCMs performed as part of the CMIP6 (under the SSP2-4.5 and SSP5-8.5 scenarios) and GeoMIP6 (under the G6sulfur and G6solar scenarios) initiatives.

The results of the spatial distribution of the potential water availability under the SSP2-4.5 and SSP5-8.5 scenarios indicate that the water reserves of countries crossed by the major Central African river basins tend to dry up under GHG increases. This drying up is reflected by a significant reduction in water availability, with the CAB undergoing the most pronounced robust changes, especially under the high-emissions scenario. It has been shown that this systematic decrease in groundwater reserves is linked to a strong projected increase in potential evapotranspiration, with among other consequences, an amplification of projected dry spells duration over the subregion (Bobde *et al* 2024, Ngavom *et al* 2024). Moreover, the results revealed that, contrary to scenario SSP2-4.5, a strong predominance towards an increase in water availability would be projected under the SSP5-8.5 scenario, with a higher amplitude expected in CB. This would suggest a simulation of heavier precipitation compared with that of potential evapotranspiration projected by the ensemble-mean models under the higher GHG-forcing scenario. The trend towards heavier precipitation simulated by the CMIP6 models under SSP5-8.5 scenario has been reported in other studies undertaken over Africa (e.g. Bobde *et al* 2024, Ngavom *et al* 2024). They attributed this behavior to the simulation by these models of a very high frequency of occurrence of days with heavy precipitation. Concerning the projected distributions of potential water availability under the SRM scenarios (G6sulfur and Gsolar), the results showed a similar pattern, but with larger (lower) spatial extents of increase (decrease). In general, the SRM scenarios discussed here result in more water availability than in their associated target scenario SSP2-4.5 (Kravitz *et al* 2015), but often not as much as in SSP5-8.5 scenario. This suggests that while mitigation of GHG emissions would be better for water availability in the Central

African river basins evaluated here, SRM is better than unabated climate change.

The seasonality of the water availability index for NB and LCB showed a deficit trend particularly during the dry season. In contrast, CAB and CB, which have a tropical climate, show a water surplus throughout the year. In the near future, the annual water availability cycles will remain consistent under the SSP2-4.5 and SSP5-8.5 scenarios, with maximum water availability during the rainy seasons. It is worth to note that compared to the baseline period, there was a slight increase in the potential water availability index over the Sahelian basins. Furthermore, in the far future, all the scenarios show a more pronounced decline in water availability over the basins located in the forested area. This could be potentially be alarming for the sustainable management of water resources, as it could have negative consequences for ecosystems and the populations that are dependent on them for their water supply. In addition, this decrease in the value of the potential water availability index was more pronounced in CAB, under the higher radiative forcing scenario. The results also showed that SRM interventions could limit the projected decrease in water availability under the high radiative forcing scenario by moving closer to the median radiative forcing or increasing it slightly.

Regarding the analysis of the year-to-year changes in the potential water availability, the results showed that in contrast to SSP2-4.5 scenario, which projects a water deficit in LCB, the SSP5-8.5 scenario projects a robust positive trend, with a moderate peak throughout the 21st century. In this river basin, the year-to-year changes in potential water availability index under the SRM scenarios showed a positive change throughout the 21st century. For the other river basins, the year-to-year changes showed a negative trend throughout the 21st century, except for NB, where a robust positive change is projected until 2050. Nevertheless, the results showed that the application of SRM techniques could lead to a reduction in the risk of water deficit in the considered river basins. This suggests that geoengineering could potentially lower the impacts of climate change by reducing water stress over Central African river basins.

Overall, the application of the SRM would increase water availability in the Sahelian basins and reduce the risk of water deficits in the forested basins. The trend towards increased water availability and, to some extent the reduction of the water deficit risk projected over the Central African river basins, could have positive impacts on food security and the livelihoods of local populations, as well as on the subregion's biodiversity and ecosystems. This could also help to reduce conflicts over access to water. However, it is important to note that the SRM also raises some concerns and uncertainties. Potential secondary effects, such as changes in precipitation patterns or disruption of local ecosystems, require particular attention. In addition, the social, economic and ethical consequences of implementing such measures must be carefully assessed.

Furthermore, it is important to note that while the study utilized projections from the state-of-the-art CMIP6 and GeoMIP6 simulations, the ensemble size of only six members may not provide a sufficiently robust quantification of uncertainties associated with the projected water deficit risks over the study area. Consequently, the results could differ by considering a larger GCMs ensemble-mean simulations or alternative model types. In addition, although this study relies on the use of the GHG-forcing scenarios SSP5-8.5 and SSP2-4.5 as references to assess the implications of the SRM experiments, recent scientific literature suggests that the level of warming prescribed by the SSP5-8.5 scenario is likely to be significantly overestimated. This implies that the real difference between SSPs and SRM scenarios could be slightly different from what is presented in this document. It should therefore be remembered that the results may be influenced by the potential bias in the radiative forcing assumptions.

In conclusion, although the SRM geoengineering may offer promising prospects for mitigating the water deficit risk over the main Central African river basins, it is important to consider the advantages and disadvantages of this technology as a whole before making an informed decision on its use. Further research, rigorous impact assessment and participatory decision-making are essential to ensure sustainable management of water resources and to minimize the undesirable side-effects of these techniques.

Data availability statement

The data that support the findings of this study are openly available at the following URL/DOI: https://esgf-metagrid.cloud.dkrz.de/search/cmip6-dkrz/.

Acknowledgments

We would like to thank the climate modelling groups listed in table 1 for producing and making their model output freely available through the Earth System Grid Federation's (ESGF) platforms. We gratefully appreciate the efforts of the LMI NEXUS along with that of the National Computing Center of Côte d'Ivoire (CNCCI) during the realisation of this work. Support for Ben Kravitz was provided in part by the National Science Foundation through agreement SES-1754740, NOAA's Climate Program Office, Earth's Radiation Budget (ERB) [grant reference NA22OAR4310479], and the Indiana University Environmental Resilience Institute. The Pacific Northwest National Laboratory is operated for the US Department of Energy by Battelle Memorial Institute under contract DE-AC05-76RL01830. Thierry C Fotso-Nguemo would like to acknowledge support from the Abdus Salam International Centre for

Theoretical Physics (ICTP) through the Associates Programme (2020–2025). Babatunde J Abiodun also acknowledges the support of the Department of Science and Technology (DST), National Research Foundation (NRF) and Centre for High Power Computing (CHPC) South Africa. Finally, the authors are grateful to the two anonymous reviewers for their recommendations and suggestions, which significantly contributed to strengthening and clarifying the initial version of the manuscript.

Funding information

The research of this article was supported by the Degrees Initiative [grant reference RGA-DMF23CMR].

ORCID iDs

Thierry C Fotso-Nguemo https://orcid.org/0000-0002-7321-9236
Steven Chouto https://orcid.org/0000-0002-4926-1039
Jean P Nghonda https://orcid.org/0000-0002-0405-3906
Arona Diedhiou https://orcid.org/0000-0003-3841-1027
Ben Kravitz https://orcid.org/0000-0001-6318-1150
Zéphirin D Yepdo https://orcid.org/0009-0006-1656-4910
Flore K Djuidje https://orcid.org/0009-0006-2544-2368
Babatunde J Abiodun https://orcid.org/0000-0002-3878-0116

References

Abiodun B J, Odoulami R C, Sawadogo W, Oloniyo O A, Abatan A A, New M, MacMartin D G, Izidine P, Egbebiyi T S and MacMartin D G 2021 Potential impacts of stratospheric aerosol injection on drought risk managements over major river basins in Africa *Clim. Change* **169** 1–19

Alterskjær K, Kristjánsson J E, Boucher O, Muri H, Niemeier U, Schmidt H and Timmreck C 2013 Sea-salt injections into the low-latitude marine boundary layer: the transient response in three Earth system models *J. Geophys. Res.* **118** 12–195

Aswathy V N, Boucher O, Quaas M, Niemeier U, Muri H, Mülmenstädt J and Quaas J 2015 Climate extremes in multi-model simulations of stratospheric aerosol and marine cloud brightening climate engineering *Atmos. Chem. Phys.* **15** 9593–610

Bobde V, Akinsanola A A, Folorunsho A H, Adebiyi A A and Adeyeri O E 2024 Projected regional changes in mean and extreme precipitation over Africa in CMIP6 models *Environ. Res. Lett.* **19** 074009

Bonou F, Da-Allada C Y, Baloitcha E, Alamou E, Biao E I, Zandagba J, Tilmes S, Pomalegni Y, Irvine P J and Tilmes S 2023 Stratospheric sulfate aerosols impacts on West African monsoon precipitation using GeoMIP models *Earth's Future* **11** e2023EF003779

Boucher O *et al* 2020 Presentation and evaluation of the IPSL-CM6A-LR climate model *J. Adv. Model Earth Syst.* **12** e2019MS002010

Camilloni I, Montroull N, Gulizia C and Saurral R I 2022 La Plata basin hydroclimate response to solar radiation modification with stratospheric aerosol injection *Front. Clim.* **4** 763983

Collins M, Knutti R, Arblaster J, Dufresne J L, Fichefet T, Friedlingstein P and Wehner M 2013 Long-term climate change: projections, commitments and irreversibility *Climate Change 2013: The Physical Science Basis. Contribution of Working Group I to the Fifth Assessment Report of the Intergovernmental Panel on Climate Change* ed T F Stocker, D Qin, G-K Plattner, M Tignor, S K Allen, J Boschung, A Nauels, Y Xia, V Bex and P M Midgley (Cambridge University Press)

Dagon K and Schrag D P 2016 Exploring the effects of solar radiation management on water cycling in a coupled land-atmosphere model *J. Clim.* **29** 2635–50

Danabasoglu G 2019 IPCC DDC: NCAR CESM2-WACCM model output prepared for CMIP6 CMIP. world data center for climate (WDCC) at DKRZ (https://doi.org/10.26050/WDCC/AR6.C6CMNRCESWA)

Eyring V, Bony S, Meehl G A, Senior C A, Stevens B, Stouffer R J and Taylor K E 2016 Overview of the coupled model intercomparison project phase 6 (CMIP6) experimental design and organization *Geosci. Model Dev.* **9** 1937–58

Greve P and Seneviratne S I 2015 Assessment of future changes in water availability and aridity *Geophys. Res. Lett.* **42** 5493–9

Hamon W R 1963 Computation of direct runoff amounts from storm rainfall *Int. Assoc. Sci. Hydrol. Publ.* **63** 52–62

IPCC 2022 Summary for policymakers *Climate Change 2022: Impacts, Adaptation, and Vulnerability. Contribution of Working Group II to the Sixth Assessment Report of the Intergovernmental Panel on Climate Change* ed H O Pörtner, D C Roberts, M Tignor, E S Poloczanska, K Mintenbeck, A Alegría, M Craig, S Langsdorf, S Löschke, V Möller, A Okem and B Rama (Cambridge University Press)

Jones P W 1999 First-and second-order conservative remapping schemes for grids in spherical coordinates *Mon. Weather Rev.* **127** 2204–10

Joshua D O-S, Edward A A and Ofosu A 2017 Comparison of five different methods in estimating reference evapotranspiration in Cape Coast, Ghana *Afr. J. Agric. Res.* **12** 2976–85

Kadkhodazadeh M, Valikhan Anaraki M, Morshed-Bozorgdel A and Farzin S 2022 A new methodology for reference evapotranspiration prediction and uncertainty analysis under climate change conditions based on machine learning, multi criteria decision making and Monte Carlo methods *Sustainability* **14** 2601

Kingston D G, Todd M C, Taylor R G, Thompson J R and Arnell N W 2009 Uncertainty in the estimation of potential evapotranspiration under climate change *Geophys. Res. Lett.* **36** 1–6

Kravitz B *et al* 2015 The geoengineering model intercomparison project phase 6 (GeoMIP6): simulation design and preliminary results *Geosci. Model Dev.* **8** 3379–92

Kravitz B, Robock A, Boucher O, Schmidt H, Taylor K E, Stenchikov G and Schulz M 2011 The geoengineering model intercomparison project (GeoMIP) *Atmos. Sci. Lett.* **12** 162–7

Kuswanto H, Kravitz B, Miftahurrohmah B, Fauzi F, Sopahaluwaken A and Moore J 2022 Impact of solar geoengineering on temperatures over the Indonesian Maritime Continent *Int. J. Climatol.* **42** 2795–814

Latham J *et al* 2012 Marine cloud brightening *Phil. Trans. R. Soc.* A **370** 4217–62

Lhomme J P 1997 Towards a rational definition of potential evaporation *Hydrol. Earth Syst. Sci.* **1** 257–64

Lu J, Sun G, McNulty S G and Amatya D M 2005 A comparison of six potential evapotranspiration methods for regional use in the southeastern United States 1 *J. Am. Water Resour. Assoc.* **41** 621–33

Müller W A *et al* 2018 A higher-resolution version of the max planck institute earth system model (MPI-ESM1. 2-HR) *J. Adv. Mod. Earth Syst.* **10** 1383–413

Muri H, Kristjánsson J E, Storelvmo T and Pfeffer M A 2014 The climatic effects of modifying cirrus clouds in a climate engineering framework *J. Geophys. Res.* **119** 4174–91

Ngavom Z, Fotso-Nguemo T C, Vondou D A, Fotso-Kamga G, Zebaze S, Yepdo Z D and Diedhiou A 2024 Projected changes in population exposure to extreme precipitation events over Central Africa under the global warming levels of 1.5 °C and 2 °C: insights from CMIP6 simulations *Mod. Earth Syst. Environ.* 1–17

O'Neill B C *et al* 2017 The roads ahead: narratives for shared socioeconomic pathways describing world futures in the 21st century *Glob. Environ. Change* **42** 169–80

Obahoundje S, Nguessan-Bi V H, Diedhiou A, Kravitz B and Moore J C 2023 Implication of stratospheric aerosol geoengineering on compound precipitation and temperature extremes in Africa *Sci. Total Environ.* **863** 160806

Odoulami R C, New M, Wolski P, Guillemet G, Pinto I, Lennard C and Tilmes S 2020 Stratospheric aerosol geoengineering could lower future risk of 'Day Zero'level droughts in Cape Town *Environ. Res. Lett.* **15** 124007

Pinto I, Jack C, Lennard C, Tilmes S and Odoulami R C 2020 Africa's climate response to solar radiation management with stratospheric aerosol *Geophys. Res. Lett.* **47** e2019GL086047

Robock A, Oman L and Stenchikov G L 2008 Regional climate responses to geoengineering with tropical and Arctic SO_2 injections *J. Geophys. Res.* **113** 1–15

Schupfner M, Wieners K H, Wachsmann F, Milinski S, Steger C, Bittner M and Roeckner E 2021 DKRZ MPI-ESM1. 2-LR model output prepared for CMIP6 ScenarioMIP (available at: www.wdc-climate.de/ui/entry?acronym=C6_4076897)

Séférian R *et al* 2019 Evaluation of CNRM Earth system model, CNRM-ESM2-1: role of Earth system processes in present-day and future climate *J. Adv. Model. Earth Syst.* **11** 4182–227

Storelvmo T, Boos W R and Herger N 2014 Cirrus cloud seeding: a climate engineering mechanism with reduced side effects? *Phil. Trans. R. Soc.* A **372** 20140116

Sylla M B, Elguindi N, Giorgi F and Wisser D 2016 Projected robust shift of climate zones over West Africa in response to anthropogenic climate change for the late 21st century *Clim. Change* **134** 241–53

Sylla M B, Faye A, Klutse N A B and Dimobe K 2018 Projected increased risk of water deficit over major West African river basins under future climates *Clim. Change* **151** 247–58

Tan M L, Juneng L, Kuswanto H, Do H X and Zhang F 2023 Impacts of solar radiation management on hydro-climatic extremes in Southeast Asia *Water* **15** 1089

Tang Y, Rumbold S, Ellis R, Kelley D, Mulcahy J, Sellar A and Jones C 2019 MOHC UKESM1. 0-LL model output prepared for CMIP6 CMIP (World Data Center for Climate (WDCC) at DKRZ) (available at: www.wdc-climate.de/ui/entry?acronym=C6_4662099)

Terzi Ö and Keskin M E 2010 Comparison of artificial neural networks and empirical equations to estimate daily pan evaporation *Irrig. Drain.* **59** 215–25

Tilmes S, Visioni D, Jones A, Haywood J, Séférian R, Nabat P, Niemeier U, Bednarz E M and Niemeier U 2022 Stratospheric ozone response to sulfate aerosol and solar dimming climate interventions based on the G6 geoengineering model intercomparison project (GeoMIP) simulations *Atmos. Chem. Phys.* **22** 4557–79

Wang W, Li C, Xing W and Fu J 2017 Projecting the potential evapotranspiration by coupling different formulations and input data reliabilities: the possible uncertainty source for climate change impacts on hydrological regime *J. Hydrol.* **555** 298–313

Xie M, Moore J C, Zhao L, Wolovick M and Muri H 2022 Impacts of three types of solar geoengineering on the atlantic meridional overturning circulation *Atmos. Chem. Phys.* **22** 4581–97

Xu Y, Lin L, Tilmes S, Dagon K, Xia L, Diao C, Cheng W, Wang Z, Simpson I and Burnell L 2020 Climate engineering to mitigate the projected 21st-century terrestrial drying of the Americas: a direct comparison of carbon capture and sulfur injection *Earth Syst. Dynam.* **11** 673–95

Zhang X, Li J, Wang Z and Dong Q 2022 Global hydroclimatic drivers of terrestrial water storage changes in different climates *Catena* **219** 106598